Organic Electronics 37 (2016) 228–238

Contents lists available at ScienceDirect

Organic Electronics

journal homepage: www.elsevier.com/locate/orgel

Buffer layers in inverted organic solar cells and their impact on the interface and device characteristics: An experimental and modeling analysis

Suman Banerjee [a, b, 1], Shailendra Kumar Gupta [b, c, *, 1], Arjun Singh [b, c], Ashish Garg [b, c, **]

[a] Department of Physics, Indian Institute of Technology Kanpur, Kanpur, India
[b] Samtel Center for Display Technologies, Indian Institute of Technology Kanpur, Kanpur, India
[c] Department of Materials Science and Engineering, Indian Institute of Technology Kanpur, Kanpur, India

ARTICLE INFO

Article history:
Received 4 March 2016
Received in revised form
24 June 2016
Accepted 26 June 2016
Available online 11 July 2016

Keywords:
Inverted solar cell
Buffer layer
Current-voltage modeling
Capacitance-voltage

ABSTRACT

Buffer layers play crucial role in increasing the power conversion efficiencies (η) in organic solar cells (OSCs) and hence it is important to understand the underlying microscopic mechanisms behind the improvements aiding the existing qualitative understanding. In this manuscript, we have investigated the role of zinc oxide (ZnO) and molybdenum oxide (MoO_3) buffer layers on the current density - voltage (J-V) characteristics of inverted organic solar cell (IOSC) devices combining experimental results with drift-diffusion based transport modeling, on the active layer (ActL) blend of P3HT:PCBM (Poly 3-hexylthiophene (P3HT): (6, 6) phenyl C61 butyric acid methyl ester ($PC_{61}BM$)), a workhorse system with well-established device data. The results show that while ZnO alone improves the open circuit voltage (V_{OC}) significantly, use of both the ZnO and MoO_3 layers help in improving the short-circuit current density (J_{SC}), aided by contributions to exciton dissociation by both layers at the electrode ActL interface. Absence of ZnO, in particular, causes S-shaped J-V curve which is attributed to reduced surface recombination velocity of majority carriers due to hindered charge extraction and non-selectivity of carrier flow towards cathode. On the other hand, presence of MoO_3film between ActL and the anode assists in making an energetically favourable contact with ActL and improves the extraction of photo generated charge carriers. Further in conjunction with dark J-V characteristics, impedance spectroscopy (IS) carried out under dark and illuminated conditions establishes the role of buffer layers in modifying the barrier heights at the contacts and the interfacial structure.

1. Introduction

In a typical organic solar cell (OSC) devices, also called normal architecture devices, presence of poly(3,4-ethylenedioxythiophene)-poly(styrenesulfonate) (PEDOT:PSS) as a hole transport layer (HTL) leads to lower device life times under ambient conditions, attributed largely to the degradation of interface between PEDOT:PSS and the bottom electrode of indium tin oxide (ITO) [1–5]. Inverted organic solar cells (IOSCs), on the other hand, show superior atmospheric stability [6,7] where PEDOT:PSS is replaced by another buffer layer, typically ZnO. However, this modification leads to a key difference between a normal and an inverted OSC device i.e. reversed polarity of the ITO and metal electrodes; in inverted OSC devices, the electrons move to the bottom ITO electrode whilst holes move to the top metal electrode (See Fig. 1). The charge selectivity towards respective electrodes is achieved by the use of two buffer layers between the active layer (ActL) and the electrodes, called electron transport and hole transport layers (ETL and HTL respectively) in the OSC devices. In inverted OSC devices, besides ZnO, various other materials have been used as ETLs such as AZO (aluminum doped ZnO), ZTO (zinc tine oxide), IZO (indium zinc oxide), TiO_2, Cs_2CO_3, CsF_2, PbO, CdS [8–16] whilst the HTL candidate materials can be from NiO, MoO_3, V_2O_5, WO_3 (transition

* Corresponding author. Samtel Center for Display Technologies, Indian Institute of Technology Kanpur, Kanpur, India.
** Corresponding author. Samtel Center for Display Technologies, Indian Institute of Technology Kanpur, Kanpur, India.
E-mail addresses: guptsk@iitk.ac.in (S.K. Gupta), ashishg@iitk.ac.in (A. Garg).
[1] These authors contributed equally to this work.

http://dx.doi.org/10.1016/j.orgel.2016.06.031
1566-1199/

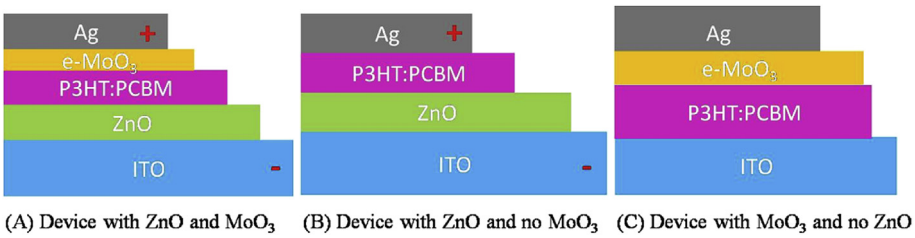

Fig. 1. Schematic representation of the three types of inverted OSC devices: device A with both the buffer layers, device B and device C without MoO_3 and ZnO layers respectively.

metal oxides), CuO_x, graphene oxides (GO) and even PEDOT: PSS [10,17–19]. The use of inverted device architecture has not only led to improved life times but also comparable power conversion efficiencies [20].

In literature, for inverted OSC devices, the role of these buffer layers has been postulated in many ways such as (i) in enhancing the optical field distribution, (ii) working as exciton blocking layers (EBL), (iii) to control the electron/hole injection and extraction in the devices, (iv) by assisting in photo-generated polaron dissociation and (v) in modifying the interfaces [21–25]. Most of these views provide a reasonable qualitative insights into the role of buffer layers in OSC devices. However, to further improve our understanding in quantitative fashion, for example, apart from being carrier selective layers, how do these layers affect carrier extraction, exciton dissociation, injection barrier and to be able to tailor the buffer layers, it would be essential to understand the underlying microscopic mechanisms. It can be a complex task due to presence of unsaturated bonds, trap distribution and any reaction layers at the interfaces.

To specifically understand the function of buffer layers, we need to quantitatively understand their effect on the microscopic parameters such as energy barrier, electron and hole density, built-in potential and electric field inside the device, the open circuit voltage (V_{OC}), effect of mobility on the device performance parameters and device capacitances for a better device design [26]. In this context, drift-diffusion based transport modeling can be a useful methodology as it has been successfully used to model the transport behavior of planar and bulk-heterojunction (BHJ) OSCs [27–29]. Although simplistic in nature, this modeling approach has been used effectively to provide us acceptable microscopic description of the device utilizing the effect of contacts [30], and minority carriers [31] on the current-voltage (J-V) characteristics as well as to explain the S-shape J-V characteristics [32] in case of OSCs.

In addition, impedance spectroscopy (IS) can be an appropriate characterization tool, especially for the analysis of electrical devices in the framework of interface/bulk studies, shedding light on the injection barriers, charge extraction, turn-on voltage, conductivity, interfacial defects and traps as well as response of charge carriers in terms of lifetime, mobility, recombination resistance, chemical capacitance and accumulation [33–36].

In this manuscript, we report the role of ZnO and MoO_3 as buffer layers on the performance of P3HT:$PC_{61}BM$ (Poly 3-hexyl thiophene (P3HT): (6, 6) phenyl C_{61} butyric acid methyl ester (PCBM)) based BHJ organic solar cell devices using a combined experimental J-V and C–V measurements and drift-diffusion based transport modeling approach. We find that the bottom ZnO layer plays an important role in affecting the exciton dissociation, injection barrier modification (built-in voltage) and mainly affects the V_{OC}. On the other hand, the top MoO_3 layer plays a critical role in interface modification for better hole collection and helps in exciton dissociation affecting the short circuit current density (J_{SC}).

2. Experimental details: device fabrication and characterization

To discern the effect of buffer layers e.g. ZnO and MoO_3, three different inverted architectures were fabricated as ITO/ZnO/P3HT:PCBM/MoO_3/Ag (Device A), ITO/ZnO/P3HT:PCBM/Ag (Device B), and ITO/P3HT:PCBM/MoO_3/Ag (Device C) depicted in Fig. 1. For devices A and B, the ETL layer of ZnO was fabricated by spin coating ZnO precursor solution (0.45 M) at 2000 rpm followed by drying at 250 °C on a hot plate for 10 min in the ambient to yield a 30 nm ZnO film. Further, ActL of P3HT:PCBM (15 mg-12 mg/P3HT:PCBM in 1 ml Chlorobenzene) was spin coated at 1500 rpm in the N_2 filled glove box followed by drying at 150 °C for 10 min to yield a 90 ± 5 nm thin film. Finally, 10 nm thick MoO_3 (for devices A and C) and 50 nm thin Ag layers were deposited by thermal evaporation using shadow mask at a deposition rate of 0.3 Å/s and 0.5 Å/s respectively. The details of process optimization can be found elsewhere [37].

The un-encapsulated devices of area, 0.09 cm^2 were characterized under 1 sun illumination on a calibrated Newport solar simulator using Keithley 2400 source-meter for J-V characteristics and IPCE (Incident photon-to-current efficiency) measurements. The impedance measurements were performed using an Agilent 4092 impedance analyzer at an AC oscillating voltage of 50 mV (rms) with measurements made in dark and at room temperature. The capacitance-voltage and impedance-frequency data were recorded at different voltages and frequencies. The photo-luminescence (PL) measurements were made (Jobin-Yyon-Spex spectrophotometer) on the P3HT:PCBM films with and without buffer layers: P3HT:PCBM on ZnO coated ITO/Glass, on ITO/Glass, and with and without evaporated MoO_3 layers on top.

3. Modeling details

The J-V model is built by numerically solving the Poisson and continuity equations [38], as shown below,

$$\frac{\partial^2 V}{\partial x^2} = \frac{q_e}{\varepsilon}[n(x) - p(x)] \tag{1}$$

$$\frac{1}{q_e}\frac{dJ_n}{dx} = R - G \tag{2}$$

$$\frac{1}{q_e}\frac{dJ_n}{dx} = -(R - G) \tag{3}$$

where q_e is the charge of electron, ε is the dielectric constant of the material, $V(x)$ is the potential and $n(x)$ and $p(x)$ are the electron and hole concentration inside the device, G and R are the generation and recombination rate. The electron and hole current density (J_n and J_p respectively) are given by,